Eur. Phys. J. Plus (2016) **131**: 19
DOI 10.1140/epjp/i2016-16019-5

THE EUROPEAN PHYSICAL JOURNAL PLUS

Regular Article

The Jülich high-brilliance neutron source project*

U. Rücker[1], T. Cronert[1], J. Voigt[1], J.P. Dabruck[2], P.-E. Doege[2], J. Ulrich[2], R. Nabbi[2], Y. Beßler[3], M. Butzek[3], M. Büscher[4], C. Lange[5], M. Klaus[5], T. Gutberlet[1,a], and T. Brückel[1]

[1] Jülich Centre for Neutron Science, Forschungszentrum Jülich GmbH, Jülich, Germany
[2] NET, RWTH Aachen, Aachen, Germany
[3] ZEA-1, Forschungszentrum Jülich GmbH, Jülich, Germany
[4] Peter Grünberg Institut, Forschungszentrum Jülich GmbH, Jülich, Germany
[5] Technische Universität Dresden, Institut für Energietechnik, Dresden, Germany

Received: 23 November 2015
Published online: 29 January 2016 –

Abstract. With the construction of the European Spallation Source ESS, the European neutron user community is looking forward to the brightest source worldwide. At the same time there is an ongoing concentration of research with neutrons to only a few but very powerful neutron facilities. Responding to this situation the Jülich Centre for Neutron Science has initiated a project for a compact accelerator driven high-brilliance neutron source, optimized for neutron scattering on small samples and to be realized at reasonable costs. The project deals with the optimization of potential projectiles, target and moderator concepts, versatile accelerator systems, cold sources, beam extraction systems and optimized instrumentation. A brief outline of the project, the achievements already reached, will be presented, as well as a vision for the future neutron landscape in Europe.

1 Introduction

With the construction of the ESS, the European neutron user community is looking forward to the brightest neutron source worldwide. At the same time there is an ongoing concentration of research with neutrons to only a few but very powerful neutron facilities. These bright lighthouses mainly serve the needs of a limited amount of experienced experimentalists, but the smaller or medium flux sources necessary for method development, user recruitment and user education, mere capacity, proof-of-principle experiments or operation of specialized instruments and methods seem to vanish.

Responding to this situation the Jülich Centre for Neutron Science has started a project towards the development and design of compact accelerator driven high-brilliance neutron sources as an efficient and cost effective alternative to current low- and medium-flux reactor and spallation sources. Such compact sources have the potential to fill the gap for the access of science and industry to neutrons and serve as local national or regional international medium-flux, but high-brilliance neutron facilities. The goal of the project is to deliver a "High-Brilliance Neutron Source (HBS)", where a compact neutron production system and a compact moderator produce a field of thermal and cold neutrons with high brilliance that can efficiently be extracted in an optimized neutron transport system.

Traditionally, neutron sources are optimized to deliver highest neutron current –or integral flux– in order to be able to serve many instruments by one moderator. This concept is also realized at the ESS, which will be the leading neutron source worldwide. In contrast, the HBS project aims at maximizing the brilliance of single neutron beams, where brilliance B is defined as

$$B = \frac{\text{neutrons}}{\text{s} \cdot \text{mm}^2 \cdot \text{mrad}^2 \cdot 0.1\% \frac{\Delta E}{E}} \,.$$

Source brilliance is given by the neutron current (number of neutrons emitted per second), normalized to the source area and the solid angle at which the neutrons are emitted. The significance of this quantity stems from Liouvilles

* Contribution to the Focus Point on "Compact accelerator-driven neutron sources" edited by C. Andreani, C.-K. Loong, G. Prete.

[a] e-mail: `t.gutberlet@fz-juelich.de`

theorem, which states that for conservative movements, the volume in phase space is conserved. This implies for conservative neutron optics that the brilliance cannot be enhanced by any optical device: loss-less optics can at most conserve brilliance.

Typical problems in science and industry mostly require a maximization of the brilliance of a neutron beam. As an example the determination of the exact position of hydrogen atoms in protein structures needs a high flux of cold neutrons to illuminate a small protein single crystal of usually less than $1\,\mathrm{mm}^3$ with a well-collimated beam. The same holds for an experiment in which the magnetic structure of an ordered ensemble of magnetic nanoparticles, a so called mesocrystal, is being studied. In both cases the samples available are tiny and high brilliance is needed for a successful experiment to deliver highest flux with low divergence in a small beam diameter. Another example can be provided by engineering or geoscience applications, where the local strain or texture in a sample is being detected by scanning with a fine, well collimated beam.

With shaping the experiment from the source to the instrument detector a dedicated holistic neutron experiment could be set-up to fulfill the different scientific requirements in a flexible and efficient way at demand by the neutron user. In order to respond to such requirements, we propose a novel type of neutron facility on the basis of flexible compact accelerators with dedicated target and moderator solutions for specific experimental requirements.

2 Characteristics and development of HBS

2.1 Nuclear reaction and target for primary neutron generation

The production of primary neutrons can be achieved by many different nuclear reactions [1]:

- In research reactors a chain reaction of nuclear fissions is maintained. Each fission process produces on average about 1 useable neutron with a heat release of 180 MeV per neutron. Mainly due to complicated nuclear licensing procedures, it is unlikely that future neutron sources in Europe are based on the fission process.
- Fusion (D-T in solid target) is used for small portable neutron generators. However with a low neutron yield of neutrons per 400 keV Deuteron with a heat release of 10000 MeV per neutron, this process seems not competitive for a higher-brilliance source.
- Spallation is the most efficient process. Protons in the GeV range hit a heavy metal target (*e.g.* Pb, W, Hg, U), where they produce around 20 neutrons per proton with a heat release of some 30 to 50 MeV per neutron. The high neutron yield combined with the relatively small heat release makes spallation an ideal choice for a source optimized for high integral flux although the interaction zone is elongated to several 10 cm due to the high energy of the protons. This hampers the coupling of neutrons efficiently into a compact moderator.
  Another drawback is that the accelerator for a high-power source becomes very expensive and a heavy steel monolith is needed for shielding of the high energy particles which are created in the spallation process. Therefore it is worthwhile to consider alternative accelerator driven neutron sources operating at lower energies.
- There are several nuclear reactions which produce neutrons by bombardment of a target material with medium energy proton or deuterium beams in the range of 2 to 50 MeV on light elements as Li or Be. Their efficiency is around 10^{-2} n/p (or per d) with a heat release of around 1000 MeV per neutron (for details see below). While much less efficient than spallation, these processes allow building a compact source at reasonable cost and by optimizing the entire setup from ion source to neutron detector, these sources become very competitive, as will be shown in this article.
- Also electrons with energies between 10 MeV and 100 MeV are used to generate neutrons via bremsstrahlung and the nuclear photo effect in the “giant dipole resonance” (GDR) region with similar efficiencies than the process described above.

The neutron efficiency and the characteristics of the neutron beam generated using ion or electron accelerators considerably depend on the target material and its configuration as well as on the energy of the primary ions and electrons respectively, and is hence a matter of optimization for a HBS. For this aim comprehensive simulation work and parameter studies were performed based on a set of models for the primary ion or electron target configurations and the connected moderator-reflector system to produce thermal and cold neutrons at HBS [2]. Figure 1 shows the cross sections of neutron producing nuclear reactions of deuterons bombarding a Be target.

Accordingly (obtained on the basis of the TENDL nuclear data library and MCNPx) the most efficient nuclear interaction for neutron emission is the nuclear stripping effect with low energy deuterons (d, n) when using Be as target material. The break-up reaction (d, n+p) also contributes significantly to the neutron release with the maximum yield at 30 MeV deuteron energy. Figure 2 shows the effect of the material in terms of neutron yield for light and heavy elements as a function of the energy of the deuteron beam. We found that ^{11}B exhibits the highest neutron yield but more work has to be done regarding mechanical engineering and heat load aspects. According to the current state of the art we will make use of beryllium as the target material.

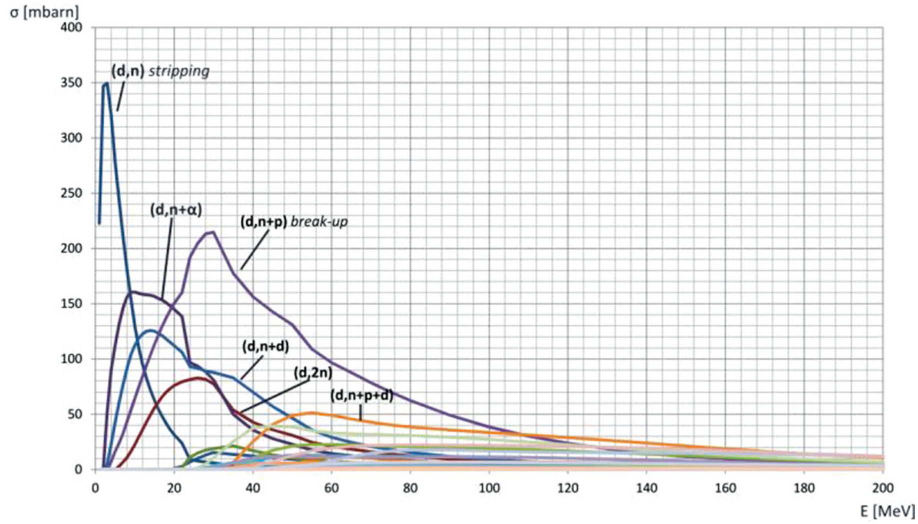

Fig. 1. Energy dependence of the cross sections of different neutron emitting reactions for deuterons impinging on Be.

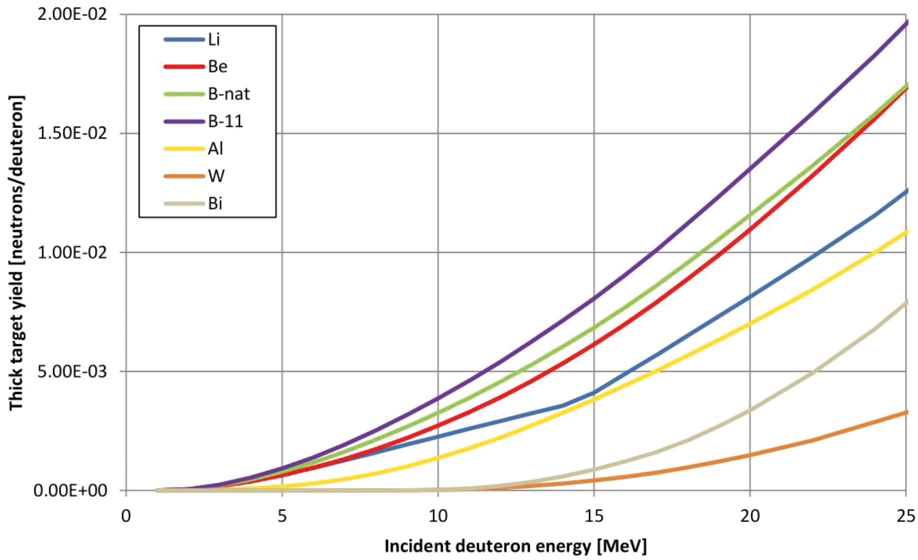

Fig. 2. Efficiency of different target materials for neutron yield as a function of the energy of deuterons.

The characteristics of the electron induced neutron production using mid-energy electron accelerators were studied with simulations based on the MCNP6 code with photonuclear data tables from ENDF-VII for different target materials and incident electron beam energies as well as the associated side effects like heat deposition and radiation damage in the target. Figure 3 shows the neutron yield (normalized to the accelerator power) as a function of electron energy for different target materials in a thick target geometry. Heavy elements, especially uranium, are obviously more suitable as photonuclear target materials due to more efficient bremsstrahlung production and the GDR region shifted towards lower energies. Beyond a certain electron energy (approx. 30 MeV) the yield per kW becomes saturated.

The effect of the target size for uranium target with cylindrical geometry is depicted in fig. 4 for different incident electron energies. In the case of 100 MeV a 2.5 cm thick uranium target would deliver optimum yield corresponding to a fraction of 5% per initial electron.

In table 1 the results of studies and simulations regarding primary neutron production are summarized. For comparison purposes the efficiency of the target concepts in terms of yield per mA and kW of the accelerator is given including the respective energy release of the nuclear reaction. Neutron beams are produced most efficiently by the Be(d, n) process and the bremsstrahlung-induced GDR process in heavy elements (U, W, Ta) in case of using a mid-energy electron beam. In spite of higher neutron efficiency, the uranium target is associated with undesirable side effects like activation and the formation of fission products which require particular long term control of the target.

Table 1. Comparison of the primary neutron production efficiencies of different incident ions and target materials. Simulations with protons and deuterons are performed using the TENDL 2014 data library. ENDF-VII data sets for protons are also available and lead to a slightly higher neutron yield. Simulations with TENDL data better fit to the experimental results given in [3].

	E[MeV]	n/ion	n/(s mA)	n/(s kW)
p ⇒ Be	5	0.02%	9.49E+11	1.90E+11
	15	0.11%	6.86E+12	6.86E+11
	25	0.64%	3.98E+13	1.59E+12
	50	2.60%	1.62E+14	3.24E+12
	100	9.79%	6.11E+14	6.11E+12
d ⇒ Be	5	0.06%	3.94E+12	7.89E+11
	15	0.26%	1.65E+13	1.65E+12
	25	1.61%	1.00E+14	4.02E+12
	50	5.72%	3.57E+14	7.15E+12
	100	19.60%	1.22E+15	1.22E+13
p ⇒ Li	2	0.002%	1.02E+11	5.11E+10
	5	0.05%	3.15E+12	6.30E+11
	10	0.16%	1.02E+13	1.02E+12
	25	0.47%	2.94E+13	1.18E+12
e ⇒ U	20	0.40%	2.47E+13	1.24E+12
	50	2.52%	1.57E+14	3.15E+12
	100	5.70%	3.55E+14	3.55E+12
	150	8.71%	5.44E+14	3.62E+12
	200	11.86%	7.40E+14	3.70E+12
e ⇒ Ta	50	1.40%	8.74E+13	1.75E+12
e ⇒ W	50	1.50%	9.36E+13	1.87E+12

In this respect W and Ta are considered as the reasonable option. In what follows, we assume neutron production by a low energy deuteron beam on a thin Be target. For this process, a particularly efficient coupling of the produced neutrons into a thermal moderator can be realized, as discussed below.

2.2 Accelerator

Compact accelerators to create a high-intensity deuteron beam have been demonstrated by various projects. At the IFMIF linear proton accelerator LIPAc a prototype for acceleration of a 125 mA deuteron beam has been constructed for 9 to 40 MeV beams, providing a deuteron beam of 1 MW beam power [4]. A similar powerful accelerator for protons is under construction at ESS Bilbao [5]. The pulse length and pulse frequency of modern accelerators can be chosen within a wide range and thus be adapted to the requirements of the neutron source instrumentation. Moreover, the beam can be distributed to different target stations by means of a multiplexer, so that one single linac can serve several target stations with individual pulse patterns. Such versatile accelerators can be used to test and optimize the neutron production.

Assuming a deuteron beam at 25 MeV, 100 mA D^+ current and 4% duty cycle the heat load on one target is 100 kW, which is the order of magnitude which we consider to be feasible concerning target cooling. The average production rate of primary neutrons at such a source would be $4 \cdot 10^{14}$ n/s, with a peak production rate of $1 \cdot 10^{16}$ n/s.

We have also considered laser-driven particle accelerators for neutron production [6]. While this might well be the method of choice in the future, we consider the technique to be not yet ripe for reliable operation of a user facility.

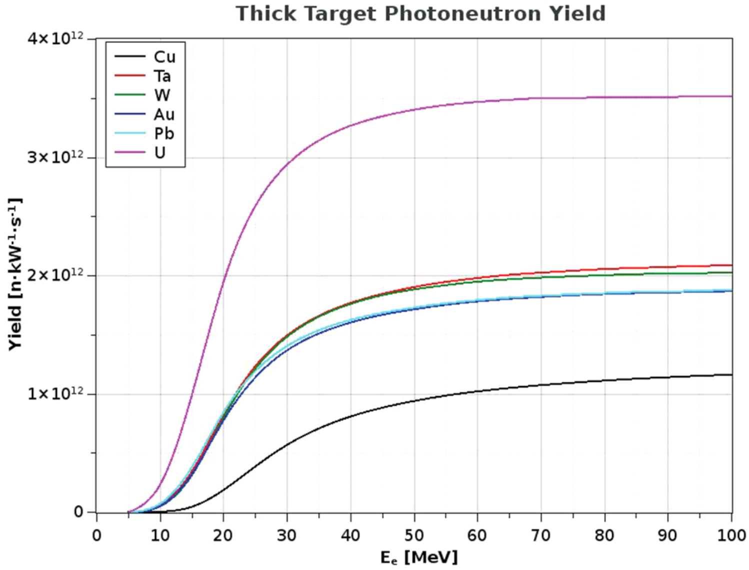

Fig. 3. Neutron yield (per kW power of an electron accelerator) for different materials for an electron beam as a function of the electron energy.

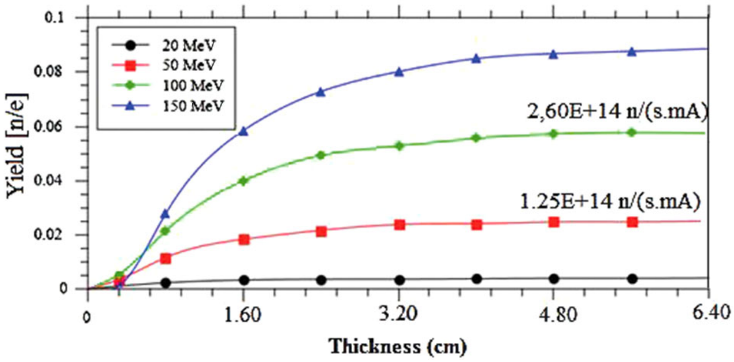

Fig. 4. Simulation of the neutron yield (per incident particle) for a uranium target for different electron energies as a function of target length.

2.3 Target

The flux and energy of accelerated particles are (for our application) just limited by the costs of the particle accelerator. Thus the amount of neutrons produced at any accelerator-driven facility (spallation as well as nuclear reaction) is limited by the thermal heat load which is accepted at the target and considerable resources have been invested into this problem during the course of accelerator driven neutron source development in the last decades.

In the course of choosing a suitable target for the HBS project the main goal is not to increase the cooling capabilities (and thus the integral flux), but to tailor the geometry of the target to be able to couple the primary neutrons efficiently into the thermal moderator.

Three different Be target designs are already published by international groups optimized to different aspects:

- At Legnaro National Lab (Italy) a compact, wedge-shaped multipurpose target has been designed and built, which can be operated with a water cooling circuit up to 150 kW thermal power [7]. As this target has been built of massive Be brazed on Cu cooling tubes, the proton beam is being stopped inside the Be bulk. Be has a very low permittivity for H_2 gas molecules, so that H_2 gas voids form inside the Be bulk. The surface of the target has been found damaged by blistering within a few weeks of operation.
- ESS Bilbao (Spain) has designed a target wheel with water cooled Be plates to improve the target cooling capability of a pulsed neutron source while keeping the geometrical origin of the neutron beam compact [8,9]. The H_2 blistering problem has so far only been discussed in theory.
- At RIKEN (Japan) a small compact neutron source with a 7 MeV proton LINAC at 700 W power is in full operation. According to their thermal load and energy, a layered target design with a Be top layer, where the neutrons are produced, and a V basis, in which the protons are stopped, was developed and patented [10,11]. As the permeability for H_2 in V is high, no voids are formed and the H_2 gas can escape through the cooling circuit. This target has been in operation for 2 years now without any signature of fatigue or damage.

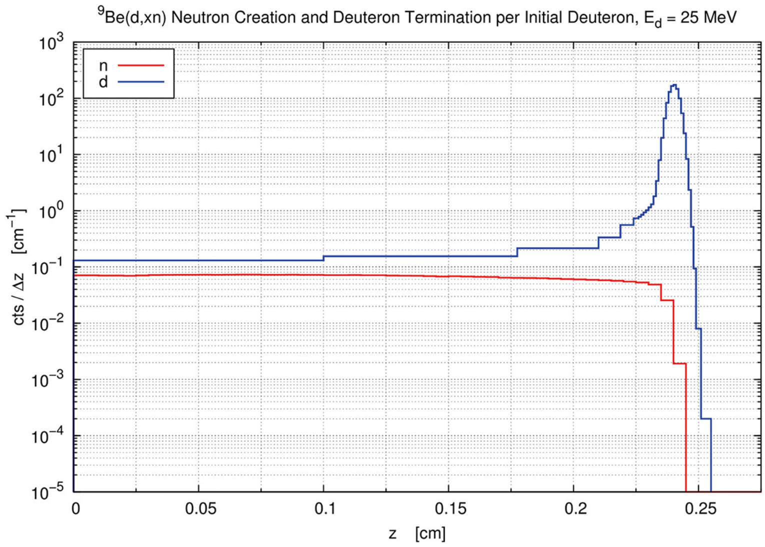

Fig. 5. Depth dependence of neutron production and D^+ ion stopping probability for a 25 MeV deuteron beam on a bulk Be target. 99% of primary neutrons are produced up to a penetration depth of 0.225 cm while 0.2% of deuterons are deposited.

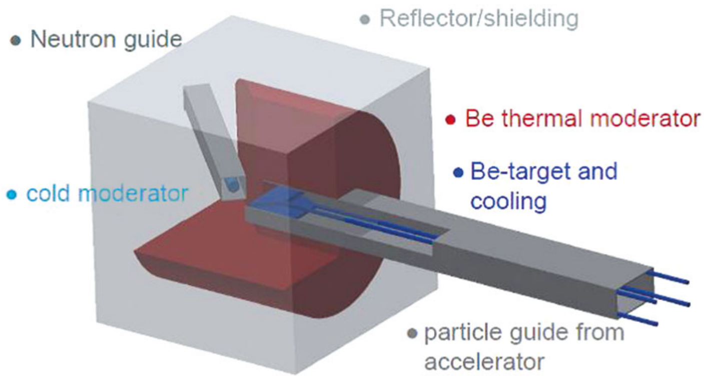

Fig. 6. Schematic drawing of a compact target-moderator setup with thermal and cold moderator.

Figure 5 shows the results of a MCNP simulation of the spatial distribution of neutron production and deuteron stopping events. By choosing the proper thickness of a Be layer on a suitable substrate one can achieve 99% of the neutron production with less than 1% of gas deposition in the Be matrix. Of course, the heat transfer must be realized, which is not possible with the design realized at RIKEN. This problem at the cutting edge of material science and engineering will be tackled in the near future.

2.4 Moderator and reflector system

A crucial structure in the production of useful neutrons is the target-moderator-reflector assembly to thermalize the neutrons produced in the target to the desired neutron energy. This requires an optimal geometric placement of the deuteron beam towards the target and thermal and cold moderator systems and the neutron beam delivery systems towards the neutron instrument (fig. 6). Since the heat deposition is not as high as in spallation sources liquid moderator materials are not mandatory. Thus, besides light and heavy water also materials like graphite and beryllium come into question. Simulation studies have shown that beryllium exhibits the highest thermal neutron yield due to its high (n, xn) cross sections. An optional outer layer of graphite serves as a reflector and can increase the thermal neutron yield at low cost.

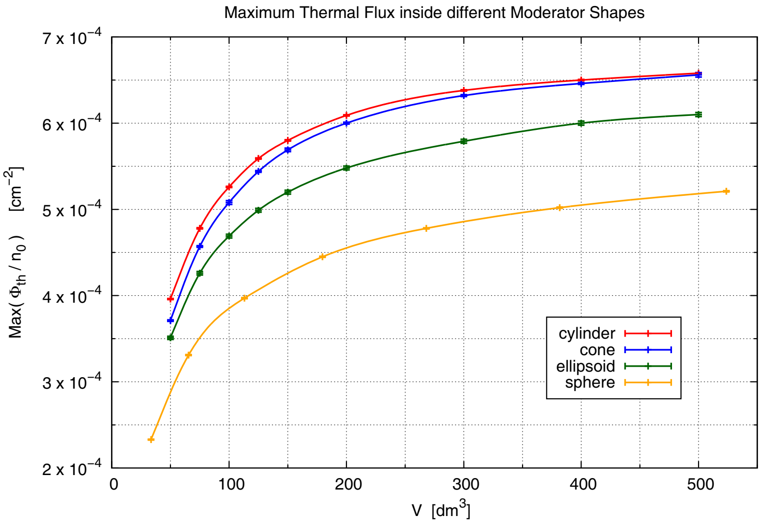

Fig. 7. Maximum thermal flux normalized to the number of primary neutrons depending on the volume of spherical, cylindrical, conical and elliptical beryllium moderators. The axes of symmetry of the moderator geometries and the beam direction of the source particles point in the positive z-direction. Since the volume of the latter three depends on two parameters, only the optimal parameter combination for a given volume is plotted.

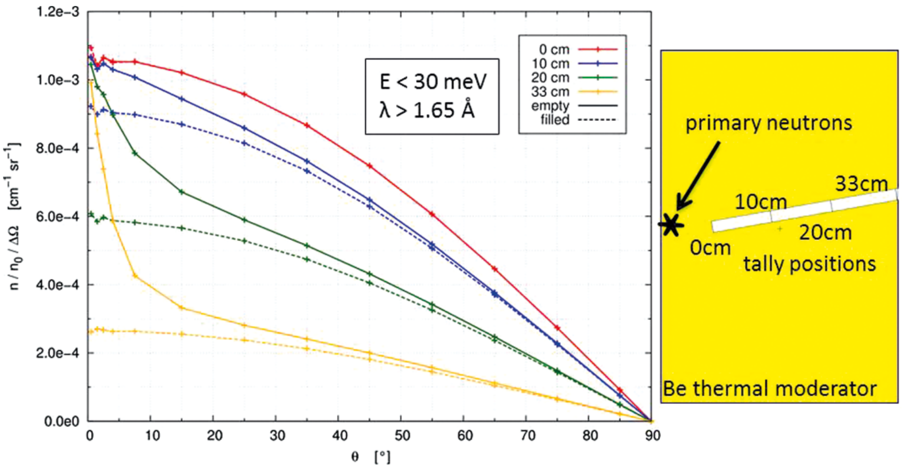

Fig. 8. Left: Angular distribution of neutrons passing a surface inside a channel at various depths for the case of an evacuated channel and a filled channel, respectively. The position at 0 cm corresponds to the bottom of the channel, while 33 cm denotes its opening. Solid lines indicate evacuated channel and dashed lines represent filled channel. Right: Corresponding MCNP geometry (cut through a cylinder). The source of primary neutrons is located on the left surface of the moderator cylinder. A vacuum channel with $r = 2\,\mathrm{cm}$ is implemented at the right moderator surface originating at the thermal flux maximum with a 10° inclination. Detector areas are defined at different depths inside the vacuum channel.

2.4.1 Moderator design

At first the influence of the outer shape of the thermal moderator on the neutron yield was studied by calculating the maximal flux of thermal neutrons ($E < 30\,\mathrm{meV}$) as a function of the moderator volume for a spherical, cylindrical, conical, and elliptical geometry (fig. 7). A cylindrical shape exhibits the highest neutron yield, where the ratio of cylinder height to radius is 1.3. As the maximum thermal flux becomes saturated for increasing volume, a reasonable approximation for the dimensions of the cylinder would be $r = 31\,\mathrm{cm}$ and $h = 41.4\,\mathrm{cm}$, which corresponds to a volume of 125 liters. These dimensions are considered in all further simulations. The maximal thermal flux is obtained on the symmetry axis of the cylinder, at a depth of 16 cm.

In the geometry shown in fig. 6, the cold moderator is placed near the thermal flux maximum, while thermal beamlines are looking to the moderator surface. In the novel designed finger moderator the extraction of thermal neutrons occurs inside the thermal moderator at the thermal flux density maximum which is realized by implementing vacuum channels into the moderator material.

The impact of such vacuum channels was investigated by means of MCNP simulations for a moderator geometry as depicted in fig. 8, right-hand side. The angular distribution of thermal neutrons ($E < 30\,\mathrm{meV}$) is calculated with respect

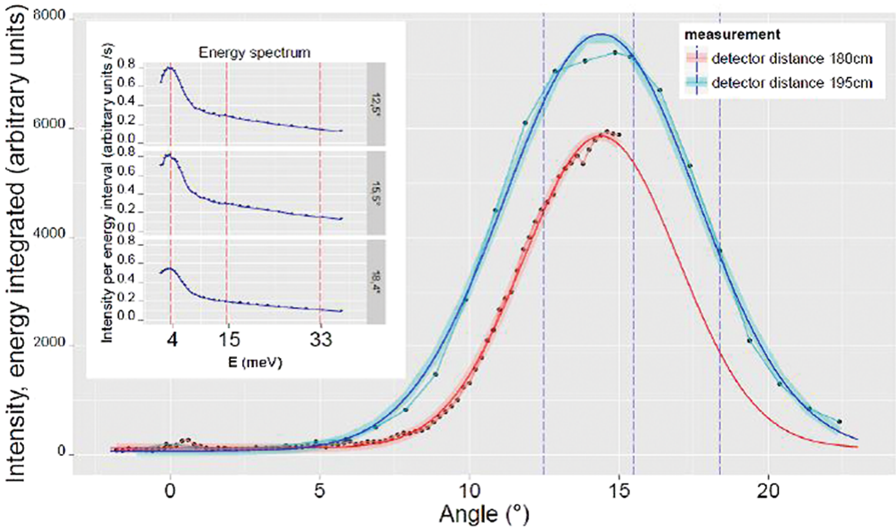

Fig. 9. Extracted thermal neutron beam of the D_2O moderator prototype at different detector distances at the TREFF beamline of MLZ.

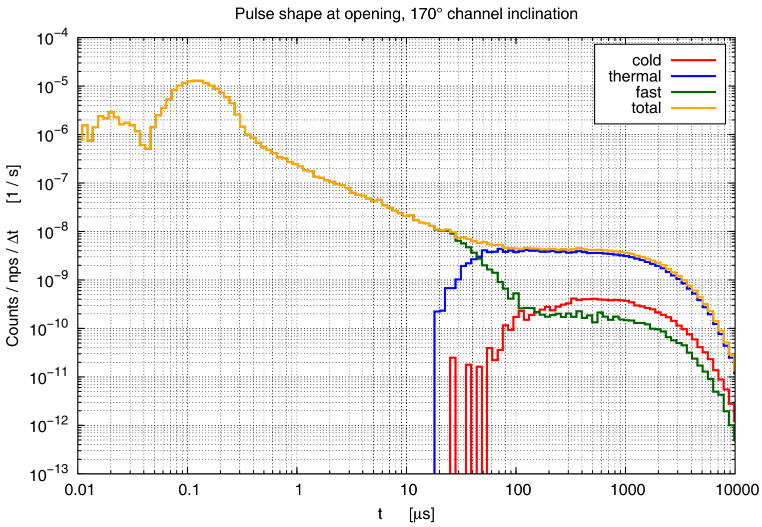

Fig. 10. Pulse shape of neutrons leaving the moderator at the channel opening. Neutrons with energy below 13.1 meV (150 K) are referred to as cold neutrons, below 127 meV (1474 K) as thermal neutrons and above as fast neutrons.

to the outwardly directed channel axis. The same calculations have been performed for the case of a channel filled with beryllium (fig. 8, left-hand side). The latter case shows that in the moderator material not only the thermal flux, but also the radial component of neutrons is significantly decreasing towards the moderator surface. This component can almost completely be preserved by implementing channels from the surface to the neutron flux maximum. In this way neutrons with appropriate flight direction to the experiment are extracted from inside the moderator instead from its surface where the amount of these neutrons is four times lower.

To test the performance of the thermal finger moderator a D_2O-based prototype was constructed and a feasibility study for the thermal finger concept performed at the TREFF neutron beamline at MLZ [12]. A highly collimated beam of cold and thermal neutrons was moderated by the D_2O reflecting moderator prototype (RMP) to thermal equilibrium and exited the moderator via the thermal finger at a 15° inclination angle (fig. 9). The initial results confirmed the calculations.

The pulse shape of neutrons leaving the moderator at the channel opening for an incident deuteron pulse of $0.2\,\mu$s based on the calculations above are depicted in fig. 10. The time structure of the pulse has been recorded for cold ($E < 13.1$ meV), thermal ($13.1\,\text{meV} < E < 127\,\text{meV}$) and fast neutrons ($E > 127$ meV) and for the entire energy range. After $100\,\mu$s the pulse consists of 90% thermal neutrons.

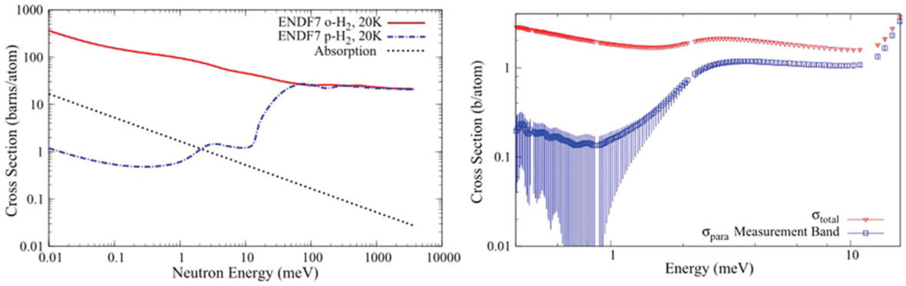

Fig. 11. Left: Scattering cross-sections for liquid ortho-H_2 (upper curve) and liquid para-H_2 (lower curve) from ENDF-VII. The para-H_2 is contaminated with a 0.5% admixture of ortho-H_2. Right: Total cross section (including scattering and absorption) and scattering cross section of pure para-H_2.

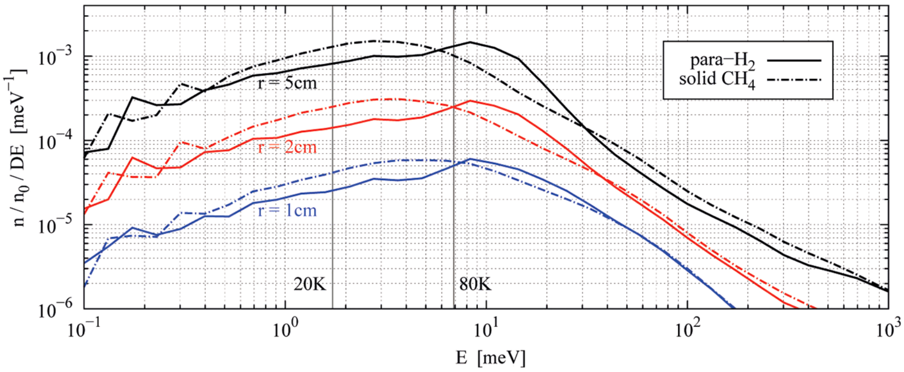

Fig. 12. Spectrum of neutrons leaving a cylindrical liquid para-H_2 or solid CH_4 moderator at 20 K for three different radii. The corresponding lengths of the cylinders are 4, 5 and 6 cm for para-H_2 and 2, 2.5 and 2.5 cm for methane.

2.4.2 Cold moderators

Typical materials for cold moderators are liquid hydrogen, liquid deuterium and solid methane. Further promising candidates are, *e.g.*, methane-clathrates or mesitylene. In a first simulation, we considered solid methane and liquid para-hydrogen as promising candidates. The H_2 molecule exists in two different nuclear spin states and is accordingly subdivided into ortho- and para-states for a triplet and singlet nuclear spin state, respectively.

In fig. 11 the total scattering cross sections of both hydrogen spin configurations are depicted. The strong increase of the neutron scattering cross section at thermal energies in para-hydrogen implies that the mean free path $L_t = 1\,\text{cm}$ of thermal neutrons is much shorter than the mean free path $L_c = 11\,\text{cm}$ of cold neutrons [13].

The thermal neutrons entering the cold moderator from the thermal Be moderator are scattered down in the cold energy region after few collisions. Due to the larger mean free path, the cold neutrons can leave the moderator without further collisions. The density of the cold neutrons is therefore higher within a layer with thickness about L_t near the moderator wall. Consequently, the optimum shape is close to a tube of length L_c and radius L_t inserted into the thermal Be moderator. Thus, the cold moderator is fed from all sides and cold neutrons which do not leave the para-hydrogen in forward direction can be reflected back by the surrounding beryllium.

In our simulations a cold moderator cylinder has been placed at the bottom of a cylindrical vacuum channel in the beryllium moderator. The optimal values for length and radius of the cold moderator at 20 K are determined in terms of the highest yield of cold neutrons in forward direction on the outwardly directed surface of the cold moderator. Because of the explanation given above ($L_c \gg L_t$ in para-hydrogen), optimal moderator shapes of para-hydrogen tend to be rod-shaped with $l = 5\,\text{cm}$ and $r = 1.5\,\text{cm}$, while solid methane's best configuration is more compact with $l = 2.5\,\text{cm}$ and $r = 1.5\,\text{cm}$. Spectra for different radii are shown in fig. 12.

Apart from the fact that solid methane delivers a higher cold neutron yield, the maximum yield in para-hydrogen is achieved at 8 meV corresponding to 90 K, while solid methane shows a smooth maximum of the cold flux between 20 K and 80 K. This can be understood by considering the steep slope around 100 K of the para-hydrogen's scattering cross section given in fig. 11. Simulations have shown, that multiple vacuum channels do not interfere with each other. Therefore the thermal Be moderator can be equipped with various cold and thermal finger moderators for various beamlines.

The MCNP calculations shown here will be validated at the AKR-2 reactor at TU Dresden, which provides a source strength of 10^8 n/s with the fission spectrum delivered to our prototype moderator surface [14]. The nominal thermal power of 2W and the relatively low flux guarantee that thermal energy transfer to the cold moderator, activation of the components used, radiation damage and tritium production in the D_2O are negligible.

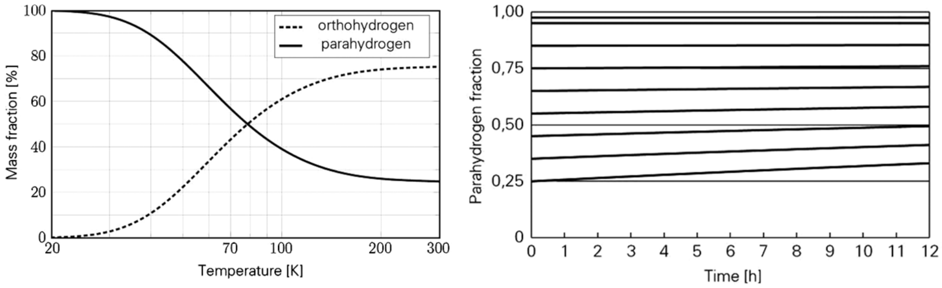

Fig. 13. Temperature-dependent thermodynamic equilibrium of ortho- to para-hydrogen mixtures (left) and change of hydrogen composition due to auto conversion over 12 hours in liquid hydrogen at 17 K and 0.15 MPa (right).

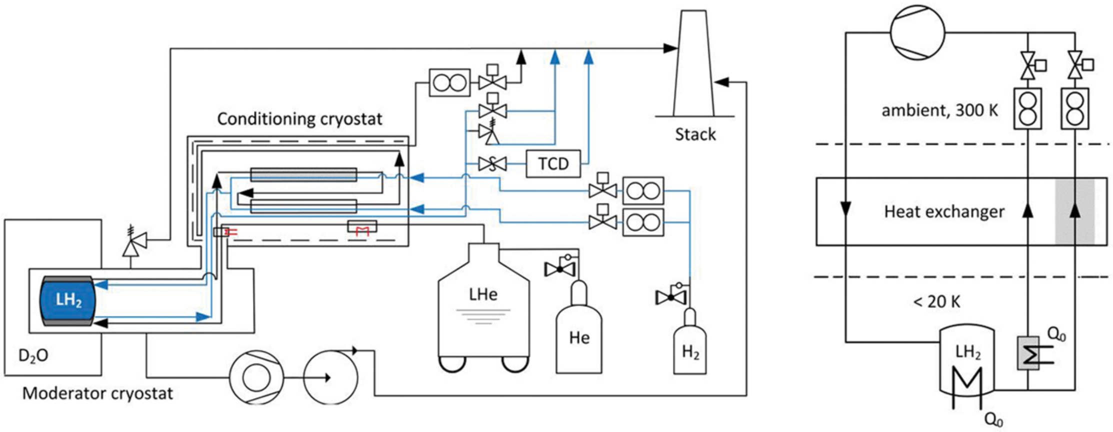

Fig. 14. Setups with adjustable ortho- to para-hydrogen composition for proof of principle (left) and for a closed hydrogen system for a HBS facility (right). The moderator vessel (ca. 0.3 liters LH_2) will be cooled externally by a helium cold gas to 17 K. Two tube-in-tube heat exchangers cool down incoming hydrogen with the exhausting helium before it finally condenses in the moderator vessel. One of the two heat exchangers will be filled with catalyst material, converting to almost pure para-hydrogen.

2.4.3 Adjustable ortho- to para-hydrogen cooling systems

To test the MCNP calculations and to be able to adjust the neutron spectrum to the needs of the experiment, an adjustable ortho- to para-hydrogen cooling system has been designed. As mentioned above the mixture of ortho-hydrogen with parallel proton spins forming three higher energy states and para-hydrogen with antiparallel proton spins as ground state will tend to its thermodynamic equilibrium ratio, which is determined by temperature only. At ambient temperatures the ortho- to para-hydrogen ratio is 3:1 and at temperatures below 20 K the equilibrium shifts to a para-hydrogen fraction of nearly one (fig. 13, left).

Two basic mechanisms of conversion can be observed. An autocatalysis caused by dipole-dipole-interactions of two ortho-hydrogen molecules leads to a change in direction of the thermodynamic equilibrium [15], which is a rather slow decelerating process. For higher ortho-hydrogen contents than equilibrium the autocatalysis has to be antagonized (fig. 13, right), which can be achieved by continuously feeding hydrogen of a higher ortho-hydrogen concentration to the system. The second, more efficient conversion mechanism is the catalysis at paramagnetic substances like transition metals and their oxides [16] used in liquefiers.

Being able to adjust and stabilize a specific hydrogen composition at low temperatures requires specific novel efforts compared to common cryogenic engineering. The task is to liquefy hydrogen and keep its temperature continuously in a narrow band (solid < 13.8 K, gaseous > 21.8 K at 0.15 MPa) in a safe manner over several hours. At the place, where the cooling power needs to be applied only aluminum is applicable. Adjusting and stabilizing different ortho- to para-hydrogen ratios concludes the set of requirements. This leads to a design as can be seen in fig. 14 to the left with two connected vacuum vessels and helium cold gas cooling from a mobile liquid helium dewar.

In the final HBS facility a closed hydrogen cycle may be preferred as indicated in fig. 14. In addition to the stabilization of favorable ortho-hydrogen contents above its thermodynamic equilibrium, this setup allows an adaption of the moderator features to the experimentalist's needs in a reasonable time.

Thermal and neutron induced para-to-ortho conversion plays a more important role the higher the total neutron flux and heat load at the target rise. These mechanics however are notoriously difficult to simulate, so that experimental data from the prototype parameter studies of the HBS can be extrapolated to larger sources (such as the ESS) and necessary information can be gained.

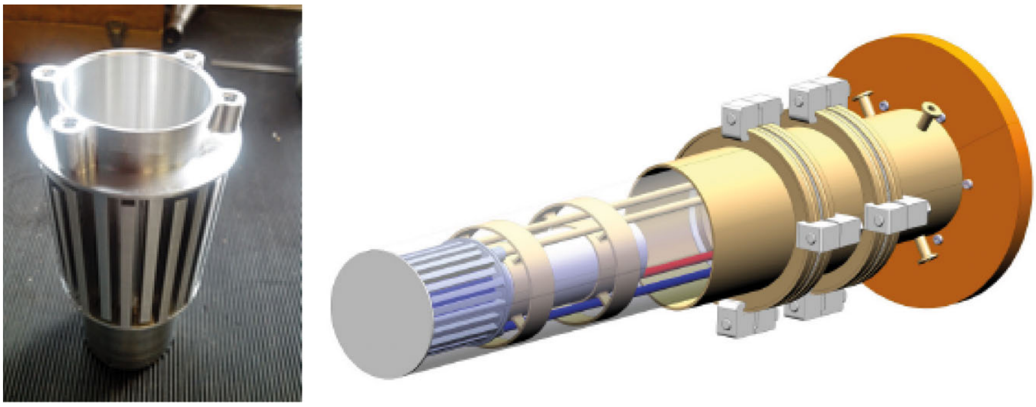

Fig. 15. Cold source prototype as developed and built for tests at the AKR-2. The cold source is a cylindrical Al vessel ($r = 25\,\text{mm}$, $l = 100\,\text{mm}$) to condense H_2 or CH_4 gas, surrounded with a He gas cooling labyrinth. The working pressure is defined as 1.5 bar for liquid H_2. The cold source is installed on a standard flange and can be inserted into an evacuated beam tube in the thermal moderator. Four gas connections are used for input and output of moderator gas and He cooling gas. On the moderator surface towards the opening of the beam tube, a filter crystal can be mounted for further treatment of the spectrum.

2.4.4 Cold moderator prototype

At the HBS each instrument can be provided with an individual cold source designed to the specific need of the corresponding instrument. The shape of the cold source can be adapted to the beam size and divergence desired at the sample position. The temperature and material can be chosen to fulfill the spectral demands of the experiment (see sect. 2.4.2).

Our present prototype of the liquid hydrogen vessel is a multipurpose source for validation studies (fig. 15). The cold finger moderator is placed inside the thermal finger, so that the cold source is directly placed within the thermal neutron flux density maximum and fed from all sides with the highest possible neutron intensity. The dimensions of the cold source are designed according to the principle of low-dimensional beam extraction proposed for the ESS cold moderator [17, 18] and the mean free path of cold and thermal neutrons in 100% para-hydrogen. The design is optimized for liquid para-hydrogen, but the condensation of gaseous methane and liquid mesitylene is also possible and varying ratios of ortho- and para-hydrogen can be investigated as well.

2.5 Beam extraction and transport

Due to the reduced radiation level and the compact target/moderator design efficient beam extraction close to the target can be achieved. The basic principle (as in conventional neutron sources) is to increase the amount of usable neutrons at the sample position, but in the concept of the finger moderator the unused neutrons are not discarded, but scattered back into the thermal moderator volume to contribute to the thermal neutron flux distribution in thermal equilibrium. The finger beam tubes are so small that the flux density inside the thermal moderator is disturbed by less than 2% (cf. red curve in fig. 8) due to the extraction of the beams for the beamlines.

With the possible extraction of the neutrons directly from the neutron flux maximum within the thermal moderator sophisticated neutron transport mechanisms can be used. These can roughly be divided into four categories: guides, lenses, filters and polarizers.

- Sophisticated neutron guide systems like elliptic or Selene neutron guides [19] profit from the smaller source as a more concentrated focal point and from the lower irradiation problems, which allows them to start directly at the focal point, within the thermal moderator.
- Neutron lenses, normally used to focus a beam at the sample, can be used directly at the source to decrease divergence and to focus the neutron beam into the guide system. Different neutron lenses at the sample position are reported to have gain factors of a magnitude and higher in flux, which in the case of the cold finger would also be true at the source position.
- Filters for fast neutrons can be implemented directly into the finger, scattering high energy neutrons back into the moderating thermal volume and allow neutrons of the desired energy range to pass out through the finger. Material like polycrystalline, cooled Be, single crystal sapphire, bismuth, MgO and silicon have been studied within the neutron community for years. Cooling can be provided by He cooling of the hydrogen vessel.
- A set of different polarization and/or monochromatization techniques could be implemented, scattering unused neutrons back into the moderating volume.

2.6 Instrumentation

Compact high-brilliance neutron sources will allow an optimized design of instruments from the source —including the moderator— to the sample and detector setup. The experimental requirements will define the parameters of source operation and construction. Modern beam transport systems will achieve brilliance transfer from the source to sample and detector with above 80% at least. Short neutron pulses according to the best detection efficiency, small beams, low fast neutron background and clean and optimized angular and spatial distribution will be achieved, *e.g.* by the concept used for the POWTEX instrument at MLZ [20], which uses an eye-of-the-needle concept with two elliptic neutron guides with octagonal cross section. The possibility to design the moderator and neutron optics specifically for each beamline, to have choppers and guides start directly from the moderator, allows a very versatile design of instruments for imaging, diffraction, large scale structures and spectroscopy. Design considerations for spectroscopy are given below.

2.6.1 Large scale structures

Instrumentation for the investigation of large scale structures typically uses small scattering angles, allowing for a low wavelength resolution. This can be achieved best, if the pulse length is long and the length of the instrument is short, so that the dispersion of the wavelengths with the flight path is less. These instruments can be supplied with cold neutrons from a compact cold source, where one or two mirrors immediately after the cold source can deflect the cold neutron beam from the direction of the fast neutron contamination inside the beamline. Depending on the desired wavelength range, the cold source can be elongated and filled with para-hydrogen for wavelengths in the range of 3 Å for a reflectometer. For a SANS instrument operating at 7 Å or more, one would choose a compact cold source filled with a large fraction of ortho-hydrogen or methane to come closer to the thermal equilibrium (cf. fig. 12). Focusing techniques will allow to properly image the small source spot of the cold moderator to the detector position, delivering a clean scattering pattern without too many losses in the collimation section and with low background.

2.6.2 Diffractometers

Diffractometers need a high wavelength resolution to be able to identify complex phases with large unit cells without superposition of Bragg peaks or Debye-Scherrer rings. The necessary resolution of down to $10^{-5} \Delta\lambda/\lambda$ cannot be achieved efficiently with the pulse structure of the target-moderator system, because the decay time of the neutron cloud inside the moderator is too long. In contrast, a double disk chopper allows to define efficiently the resolution and, by proper synchronization of the primary pulse to the chopper, the spectrum available after the chopper. For the use of hot neutrons ($\lambda = 0.5$ Å), one can choose a source time just at the end of the ion pulse, when the fast neutrons are not yet fully thermalized in the moderator. For the use of thermal neutrons ($\lambda = 1.5$ Å) one will choose to extract a neutron pulse from the equilibrium state of the thermal moderator. For high-resolution experiments on samples with smaller unit cell at longer wavelengths ($\lambda = 4$ Å) a cold source vessel inside the beamline can be filled with liquid hydrogen to supply a higher flux of neutrons in the appropriate range.

Typically, diffractometers are equipped with area detectors that cover a large range of scattering angles, so that the wavelength band used can be relatively narrow. This, together with the short pulses from the high-resolution chopper system allows for the operation of this instrument class at repetition rates of 200 Hz or higher, which can be supplied at a dedicated target station for such instruments.

2.6.3 Spectroscopy

At a pulsed source the time-of-flight technique is the method of choice for neutron energy analysis. The number of neutrons, which illuminate the sample, depends on the peak brightness of the moderator and the repetition of the sample illumination. At a continuous source the sample is usually illuminated by a monochromatic beam and the repetition rate is chosen according to the time needed to record the neutrons scattered within the dynamical range of interest. When the source frequency and repetition rate mismatch (as can be the case for instruments at spallation sources), the methods of wavelength frame multiplications and multiple E_i or repetition rate multiplication (RRM) have been invented to increase the duty cycle of the instruments at the detector. The individual pulses/frames illuminate the sample with neutrons of different energy resulting in different dynamic ranges to be probed. In particular if one aims for concentrating onto a narrow range, long instruments are needed, *e.g.* 160 to 170 m instrument length for many spectrometers at the ESS. For the high-brilliance source the higher flexibility in terms of the pulse creation allows one to use a monochromatic illumination with a matched frequency, resulting in a straight forward data treatment, visualization and interpretation. In particular instruments requiring a narrow band width can be realized very compact on such a source, *e.g.* a ToF backscattering spectrometer or direct geometry chopper spectrometer.

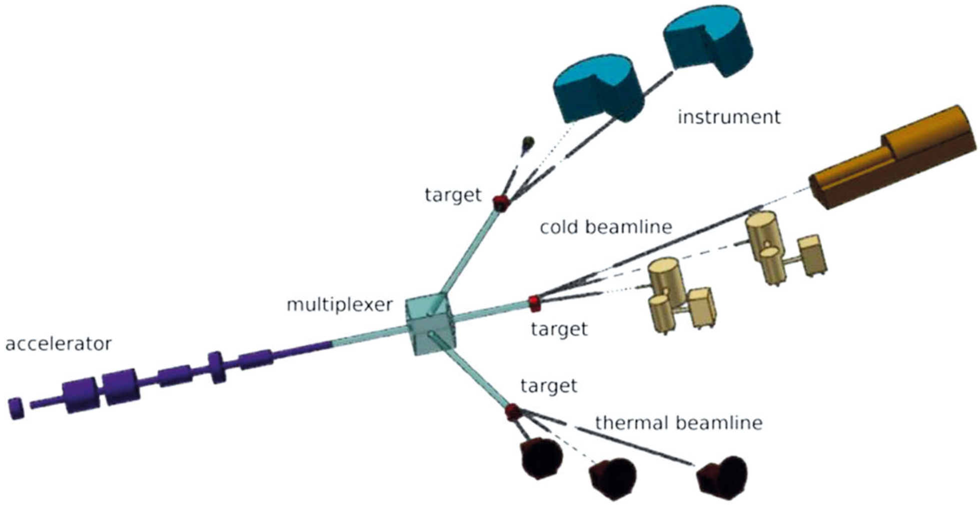

Fig. 16. Schematic layout of a future accelerator-driven high-brilliance neutron source.

The instrument design at J-PARC and the ESS has shown that the performance of the instruments can be enhanced, if the moderator pulse length is not fixing the instrument resolution, but the resolution can be set according to the experimental requirements using pulse shaping by a device, *e.g.* a neutron chopper. Therefore the instrument design requires a minimal pulse length, which does not define the instrumental resolution in the envisioned most relaxed configuration. Concentrating on compact instrument designs a 30 m for ToF- backscattering and a 20 m for a direct geometry chopper spectrometer we estimate a pulse length of 30 μs for the backscattering case and 70 μs, 250 μs and 700 μs for the chopper spectrometer for epithermal, thermal and cold neutrons, respectively. All these required pulse lengths can be prepared by choppers with existing technology from a longer pulse *e.g.* of 1 ms length. The criterion for the accelerator pulse length is hence the optimization of the moderator peak brightness.

The instruments at a compact source will benefit from the opportunity to install devices very close to the moderator. As spectrometers usually accept a wider divergence, the installation and survival of optical elements close to the moderator will lead to an enhanced tailoring of the phase space providing more useful neutrons on the sample and less background in the sample area. As the ESS promises to realize gain factors from 100 to 1000 compared to the existing instrumentation, one can expect that spectrometers at the HBS perform better than existing instruments at todays European neutron sources, if a peak brightness of 1% of the ESS can be realized.

2.7 Facility layout

A neutron scattering facility based on a high brilliance neutron source will be the result of a novel holistic approach of designing neutron scattering instruments. Already today, a neutron scattering facility comprises many different instruments from diffractometers on atomic or large scales to spectrometers with resolution between eV and neV. These instruments are fed by thermal beam tubes or secondary sources as *e.g.* a liquid H_2-cold neutron source.

The basis of the HBS facility is a target-moderator combination that offers a pulsed neutron beam at optimal frequency, pulse duration and neutron spectrum to fulfill the needs of a single instrument. Based on today's knowledge, the limitation of the peak flux will be determined by cooling issues of the compact target, so that the average power on an optimized target will be independent of the pulse frequency. This offers the opportunity to design a facility based on a dedicated ion accelerator with optimized energy and current that is multiplexed to feed several target stations that are operated at different frequencies (fig. 16). So a high-frequency target station (up to 600 Hz) can feed diffractometers and thermal chopper spectrometers, while a long-pulse target station (ca. 15 Hz) will serve instrumentation for large-scale structures that can accept larger wavelength bands $\Delta\lambda$ to increase the usable neutron flux as the wavelength resolution does not affect the Q resolution very much at small scattering angles. More target stations will serve the needs for other types of instrumentation. As the heat load is the limiting factor, all target stations will be equipped with identical targets operating at the same duty cycle. A multiplexing scheme for the accelerator will provide the ion beam for all targets from a common accelerator.

The moderators will then be optimized according to the spectral needs of the individual instruments. The thermal moderators will be optimized to provide the highest flux integrated over the timescale the instrument can accept to achieve the necessary wavelength resolution. Eventually, the pulse will be shaped with a chopper in immediate neighborhood to the moderator. Note that, compared to spallation sources, the radiation field is much smaller for an HBS type facility, which permits the placing of neutron optical elements (lenses, guides, polarizers, choppers, etc.) in direct neighborhood of the moderator. For instruments using thermal or epithermal neutrons, a finger opening in the thermal moderator will be used to extract a beam with appropriate divergence directly from the flux maximum inside the thermal moderator volume. For instruments using longer wavelengths, an appropriate cold source will be inserted into such a beam tube, shifting the neutron spectrum to the optimal temperature. The material, geometry and temperature of the cold source will be optimized for each instrument individually. For instruments operating with a narrow wavelength band it is even possible to decide from the experiment planned if cold neutrons (with cold source filled and in operation) or thermal neutrons (with the cold source empty and warm) are needed.

The number of instruments at each target station will typically be lower than 6, in order not to dilute the thermal flux maximum. Also, angular space between adjacent beamlines is necessary to be able to place choppers and other neutron optical elements close to the moderator surface. With 4 target stations being fed at different frequencies, an HBS facility can then be equipped with about 20 instruments, which is comparable to the instrumentation of a medium-flux neutron scattering facility at current research reactors.

3 Summary and conclusions

With the Jülich HBS project, we propose a novel type of neutron facility, where the neutron source, *i.e.*, moderator and beam extraction, becomes an integral part of the neutron instrument. Using low-energy nuclear reactions, the entire chain from ion source through accelerator, target, moderator, reflector, beam extraction, beam transport, instrument design up to the detector can be optimized efficiently. Examples of our ongoing optimization work have been given in this article. Our holistic approach has the potential to partly compensate for the lower efficiency of the nuclear reaction used as compared to the spallation process and offers the possibility to build compact but competitive neutron sources with an attractive price tag. Besides high end facilities, small facilities for educational purposes and less demanding experiments can be realized as a byproduct of our development (compare the JCANS network in Japan [21]). Our project aims for a novel and innovative approach enabling the establishment of a network of smaller and medium sized neutron sources in Europe based on accelerator driven facilities with low nuclear inventory and minimum invest and running costs. Such facilities address the needs of a grown European user community in science and industry, allow education and training, future effective method development and application to specific needs and requirements. The possible European network of such sources will complement the existing and future high flux neutron sources as ILL, FRM II, ISIS and ESS. The HBS project is an integral part of the Helmholtz neutron strategy [22] and has been included in the Helmholtz roadmap for research infrastructures [23].

References

1. G. Mank, G. Bauer, F. Mulhauser, Rev. Accl. Sci. Tech. **4**, 219 (2011).
2. P.-E. Doege, *MSc thesis* (RWTH Aachen, 2015).
3. S. Kamada, T. Itoga, Y. Unno, W. Takahashi, T. Oishi, M. Baba, J. Korean Phys. Soc. **59**, 1676 (2011).
4. J. Knaster, P. Cara, S. Chel, A. Facco, J. Molla, H. Suzuki, *Proceedings of IPAC2013*, 1090 (2013).
5. I. Bustinduy, F.J. Bermejo, Phys. Proc. **60**, 157 (2014).
6. M. Roth, D. Jung, K. Falk, N. Guler, O. Deppert, M. Devlin, A. Favalli, J. Fernandez, D. Gautier, M. Geissel, R. Haight, C.E. Hamilton, B.M. Hegelich, R.P. Johnson, F. Merrill, G. Schaumann, K. Schoenberg, M. Schollmeier, T. Shimada, T. Taddeucci, J.L. Tybo, F. Wagner, S.A. Wender, C.H. Wilde, G.A. Wurden, Phys. Rev. Lett. **110**, 044802 (2013).
7. J. Esposito, P. Colautti, S. Fabrisiev, A. Gervash, R. Giniyatulin, V.N. Lomasov, A. Makhankov, I. Mazul, A. Pisent, A. Pokrovsky, M. Rumyantsev, V. Tanchuk, L. Tecchio, Appl. Radiat. Isot. **67**, S270 (2009).
8. F. Sordo, S. Terron, M. Magan, G. Muhrer, A. Ghiglino, F. Martinez, P.J. de Vicente, R. Vivanco, J.M. Perlado, F.J. Bermejo, Nucl. Instrum. Methods A **707**, 1 (2013).
9. F. Sordo, F. Fernandez-Alonso, M.A. Gonzales, A. Ghiglino, M. Magan, S. Terron, F. Martinez, P.J. de Vicente, R. Vivanco, F.J. Bermejo, J.M. Perlado, J. Phys.: Conf. Ser. **549**, 012001 (2014).
10. Y. Yamagata, K. Hirota, J. Ju, S. Wang, S. Morita, J. Kato, Y. Otake, A. Taketani, Y. Seki, M. Yamada, H. Ota, U. Bautista, Q. Jia, J. Radioanal. Nucl. Chem. **305**, 787 (2015).
11. Y. Yamagata, K. Hirota, J.-M. Ju, RIKEN No. 23773, PCT/JP2013/056188 (2013).
12. S. Mattauch, U. Rücker, Schr. Forschungszent. Jülich Schlüsseltechnol. **28**, 10 (2011).
13. J. Van Kranendonk, *Solid Hydrogen* (Plenum Press, New York, 1983).
14. H. Tagaziria, W. Hansen, Rad. Protect. Dosim. **107**, 73 (2003).
15. Y. Milenko, R. Sibileva, M. Strzhemechny, J. Low Temp. Phys. **107**, 77 (1997).
16. D.H. Weitzel, W.V. Loebenstein, J.W. Draper, O.E. Park, J. Res. Natl. Bur. Stand. **60**, 221 (1958).
17. K. Batkov, A. Takibayev, I. Zanini, F. Mezei, Nucl. Instrum. Methods A **729**, 500 (2013).
18. F. Mezei, L. Zanini, A. Takibayev, K. Batkov, E. Klinkby, E. Pitcher, T. Schnfeldt, J. Neutron Res. **17**, 101 (2014).
19. J. Stahn, U. Filges, T. Panzner, Eur. Phys. J. Appl. Phys. **58**, 11001 (2012).
20. A. Houben, W. Schweika, Th. Brückel, R. Dronskowski, Nucl. Instrum. Methods A **680**, 124 (2012).
21. `http://phi.phys.nagoya-u.ac.jp/JCANS/index.html`.
22. `http://www.helmholtz.de/forschung/materie/from_matter_to_materials_and_life/`.
23. `http://www.helmholtz.de/en/research/research_infrastructures/`.